Dark Andreev states in superconductors

Andrey Grankin and Victor Galitski
Joint Quantum Institute, Department of Physics, University of Maryland, College Park, Maryland 20742, USA

(Received 22 June 2022; revised 5 December 2022; accepted 8 May 2023; published 5 July 2023)

The conventional Bardeen-Cooper-Schrieffer model of superconductivity assumes a frequency-independent order parameter, which allows a relatively simple description of the superconducting state. In particular, its excitation spectrum readily follows from the Bogoliubov–de Gennes (BdG) equations. A more realistic description of a superconductor is the Migdal-Eliashberg theory where the pairing interaction, the order parameter, and electronic self-energy are strongly frequency dependent. This paper combines these ingredients of phonon-mediated superconductivity with the standard BdG approach. Surprisingly, we find qualitatively new features, such as the emergence of a shadow superconducting gap in the quasiparticle spectrum at energies close to the Debye energy. We show how these features reveal themselves in standard tunneling experiments. Finally, we also predict the existence of additional high-energy bound states, which we dub "dark Andreev states."

DOI: 10.1103/PhysRevB.108.024501

I. INTRODUCTION

Bardeen-Cooper-Schrieffer (BCS) theory of superconductivity [1] and Bogoliubov–de Gennes (BdG) equations have proven to be relatively simple and reliable tools to describe a variety of conventional superconductors. A key simplifying assumption of this approach is that the superconducting order parameter is energy independent [2]. Although it is clearly not the case in any real superconductor, many features, such as the quasiparticle spectrum, thermodynamic, and electromagnetic properties [1,2] appear insensitive to this approximation. It is reasonable because the omitted energy dependence normally does not affect low-energy physics. In contrast, accurate determination of the transition temperature is sensitive to the details of the phonon dispersion, the dynamical screening of Coulomb interaction and the structure of the superconducting gap. The latter can be obtained from the Migdal-Eliashberg equations [3,4], which are integral equations in both energy and momentum.

This Migdal-Eliashberg theory [5] predicts a nontrivial structure of the superconducting gap as a function of *real* frequency. In particular, it was shown that for superconductivity mediated by the Einstein phonon modes [6,7], the gap function has sharp resonancelike features, such as a pole, which is located close to the real-frequency axis. Equivalently, such a pole can be interpreted as a presence of an "antivortex" [8] in a frequency-dependent gap. In the weak-coupling regime, these features can be well approximated by the Lorentz function centered at the Debye frequency. Another interesting real-frequency behavior of the gap function is discussed in Ref. [8] where the authors predict the possibility of formation of frequency-domain vortices in the presence of phonon-induced attraction and Coulomb repulsion.

In this paper, we study how a frequency-dependent order parameter affects the quasiparticle spectrum and tunneling properties of a superconductor. We assume that the frequency dependence has a Lorentz shape, which corresponds to optical-phonon-mediated pairing [4]. We solve the corresponding generalized BdG equations and show that an additional gap emerges in the qusiparticle spectrum at higher energies. In the case of a *SNS* junction, we also find that additional Andreev in-gap high-energy states can form. We note that high-energy features were also studied in the field of point-contact spectroscopy [9,10]. In contrast, in the current paper, we study the properties of quasiparticles in the presence of sharp features of the gap function. We use an analogy with quantum optics to interpret these high-energy peaks in terms of "dark" resonance features [11–13] of the BdG Hamiltonian with a frequency-dependent order parameter. This suggests a speculation that these finite-energy states could potentially be used to reliably store quantum information.

In this paper, we consider the conventional *s*-wave superconductor but keeping a complete realistic frequency dependence of the order parameter. We restrict our discussion to the mean-field level and rely on the Bogoliubov–de Gennes approach, which requires a straightforward generalization. Consider an electron gas with the creation (annihilation) operators $\psi^\dagger_{\mathbf{k},\sigma=\uparrow,\downarrow}(\psi_{\mathbf{k},\sigma})$, where $\mathbf{k}$ denotes the electron momentum. For the two-component spinor $\Psi_{\mathbf{k},n} = \{\psi_{\mathbf{k},\downarrow}(i\varepsilon_n), \psi^\dagger_{-\mathbf{k},\uparrow}(-i\varepsilon_n)\}^T$, the Green's function is defined as $\hat{\mathcal{G}}_{\mathbf{k}}(i\varepsilon_n) \equiv -\langle \Psi_{\mathbf{k},n} \otimes \Psi^\dagger_{\mathbf{k},n}\rangle$, where $\varepsilon_n = (2n+1)\pi/\beta$ is the standard of the fermionic Matsubara frequency, β is the inverse temperature, and $n \in \mathbb{Z}$. Neglecting the momentum dependence of the self-energy, the Green's function of an interacting Fermi gas can be written as [4,14]

$$\hat{\mathcal{G}}^{-1}_{\mathbf{k}}(i\varepsilon_n) = i\varepsilon_n \mathcal{Z}_n \hat{\tau}_0 - \phi_n \hat{\tau}_1 - \xi_k \hat{\tau}_3, \tag{1}$$

where $\xi_k = k^2/2m - \mu$, m is the electron mass, μ is the chemical potential, τ_i are Pauli matrices. and $\mathcal{Z}_n$ denotes the inverse quasiparticle residue obtained from the odd part of the normal-state self-energy. The off-diagonal matrix element ϕ_n stands for the anomalous self-energy. $\mathcal{Z}_n$ and ϕ_n naturally appear in both intrinsic and proximity-induced superconductors [15,16]. The BdG equations correspond to $\hat{\mathcal{G}}^{-1}_{\mathbf{k}}(i\varepsilon)\chi = 0$,

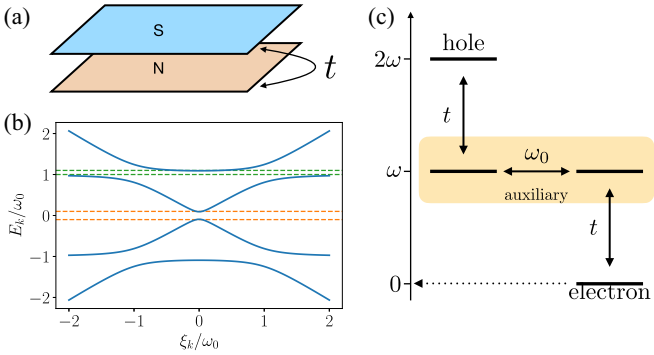

FIG. 1. (a) Effective proximity system, which induces a Lorentz-shape frequency dependence of the order parameter. The fictitious flat-band superconductor is shown in blue, and a normal-state metal is shown in orange. (b) Quasiparticle spectrum of the BdG equation with the frequency-dependent order parameter. Additional band gaps are formed close to the characteristic frequency of the order parameter frequency dependence. Blue solid lines correspond to the eigenenergies of Eq. (3). Orange dashed stands for the conventional BCS gap ($\pm\phi_0$), and dashed green lines $E_k = \omega_0$ and $E_k \approx \omega_0 + \phi_0$ correspond to the additional gap due to the frequency dependence of the order parameter. In the simulation, we assumed $\phi_0 = \omega_0/10$. (c) Schematic of the four-state system equivalent to the on-shell quasielectron branch of the BdG Hamiltonian Eq. (4) in the limit of weak-coupling $t \to 0$.

which parametrically determines the sought-after quasiparticle dispersion (here, χ is a Nambu spinor).

To calculate the quasiparticle spectrum, we need an explicit form of the frequency dependence of the anomalous self-energy. In what follows, we consider the aforementioned Lorentz-shaped form (parametrized by its amplitude ϕ_0 and the characteristic frequency ω_0)

$$\phi_n = \phi_0 \frac{\omega_0^2}{\varepsilon_n^2 + \omega_0^2}. \tag{2}$$

As demonstrated in Refs. [6,7] this solution naturally appears in superconductors where pairing is induced by an optical phonon mode with the Einstein spectrum at weak coupling. We now consider the spectrum of quasiparticles in Eq. (1).

To develop intuition, it is instructive to consider an auxiliary setup, which involves a fictitious flat-band superconductor with a frequency-independent gap proximity coupled to a normal metal as shown in Fig. 1. As we show, a proper choice of parameters in this setup gives rise to a Green's function, which replicates Eq. 1 with the order parameter (2). The advantage of this construction is that its BdG Hamiltonian below involves only standard, frequency-independent parameters,

$$\hat{\mathcal{G}}_k'^{-1}(i\varepsilon_n) = i\varepsilon_n \hat{\tau}_0\hat{\sigma}_0 - \hat{H}_{\text{BdG}} \tag{3}$$

$$H_{\text{BdG}} = \xi_k \hat{\tau}_3 \frac{(\hat{\sigma}_3 + \hat{1})}{2} - \omega_0 \hat{\tau}_1 \frac{(\hat{1} - \hat{\sigma}_3)}{2} + t\,\hat{\tau}_3\hat{\sigma}_1, \tag{4}$$

Her, $\hat{\tau}_i$ represents Pauli matrices in the Nambu space, and $\hat{\sigma}$ parametrizes an effective two-band model: $(\hat{\sigma}_3 + \hat{1})/2$ projects on the normal metal fermion modes and $(\hat{1} - \hat{\sigma}_3)/2$ projector on the fictitious flat-band superconductor. The order parameter in the latter is set the characteristic phonon frequency ω_0. We note that we assumed no intrinsic order parameter for the original fermions. The coefficient t denotes the tunneling amplitude between the superconductor and the metal. The auxiliary superconductor can be integrated out generating both the anomalous and the normal self-energies. By choosing $t = \sqrt{\phi_0\omega_0}$, we can exactly match frequency dependence of the order parameter to reproduce Eq. (2). The corresponding $\mathcal{Z}$ factor in Eq. (1) is equal to $\mathcal{Z}_n = [1 + \phi_0\omega_0/(\omega_0^2 + \varepsilon_n^2)] \approx 1$ for $\phi_0 \ll \omega_0$. This procedure effectively replaces the integrating out the bosonic Einstein-phonon degree of freedom (which generates the frequency dependence of the gap in the physical setup) with the integrating out the degrees of freedom of the auxiliary flat-band superconductor. Note that this picture is introduced for the purposes of illustration only. All results can reproduced in the original model directly. As we discuss in the Supplemental Material (SM) [17], the inverse quasiparicle residue, $\mathcal{Z}_n$ cannot be set identically to one because it would result in an unstable spectrum.

The quasiparticle spectrum can now be found by diagonalizing the static BdG Hamiltonian H_{BdG} given in Eq. (4). The result is shown in Fig. 1(b), and it has two band gaps. First, we observe the conventional BCS-like band gap at low frequencies $[-\phi_0, \phi_0]$. It can be obtained by, e.g., neglecting the frequency dependence of the self-energy in Eq. (1), which reduces it to the textbook case. The second band gap at high energies is a specific feature of the two-band system as defined in Eq. (3). As a result of the flatness of one of the dispersion relations, the avoided crossing forms a band gap close to the frequency ω_0. The value of this second band gap can be readily obtained analytically from Eq. (3),

$$\phi_2 = \sqrt{\frac{\omega_0}{2}\left[\sqrt{\omega_0(4\phi_0 + \omega_0)} + \phi_0 + \frac{\omega_0}{2}\right]} - \omega_0 \approx \phi_0, \tag{5}$$

where the approximate sign corresponds to the limit $\phi_0 \ll \omega_0$, which must hold for weak coupling.

We now define the local density of states (LDOS) of the electron gas as $\frac{-1}{\pi}\int d\xi_k \text{Im}[G_{\mathbf{k}}(\omega + i0^+)]_{1,1}$, where $G_{\mathbf{k}}$ is the Green's function 3 analytically continued to real frequencies. As the direct consequence of the band gap, the LDOS is strongly depleted at frequencies $\approx[\omega_0, \omega_0 + \phi_0]$ as shown in the inset in Fig. 2. We note that the exactly zero density of states is a feature of the flat-band dispersion of the auxiliary superconductor/Einstein phonons. However, as we discuss in the SM, the introduction of a finite curvature to the phonon dispersion would still lead to a significant depletion of the density of states. As we discuss below, this secondary gap can host additional Andreev [18] reflection peaks, observable in metal-superconductor heterostructures.

We now explore how the additional sharp Lorentz-like features of the gap function affect the superconducting proximity effect. In order to describe the transmission and reflection of quasiparticles, we employ the Blonder-Tinkham-Klapwijk (BTK) formalism [19]. We consider a heterostructure consisting of semi-infinite normal and superconducting metals (NS) with the junction located at $z = 0$ as shown in Fig. 3. Following Ref. [19], we consider the scattering of an incident electron off of the barrier. The strength of the proximity effect

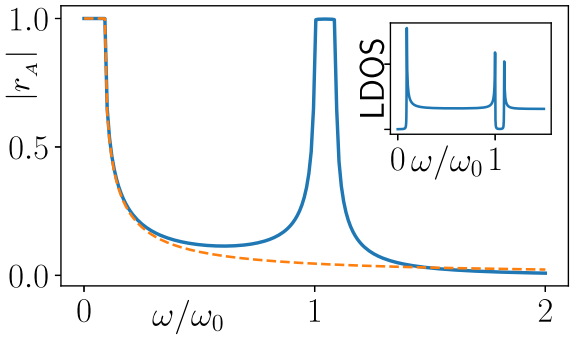

FIG. 2. Andreev reflection coefficient as function of the incident electron frequency assuming $H = 0$. As result of the additional band gap, the additional Andreev reflection peak is observed at frequencies close to ω_0. The blue solid line corresponds to the BdG equation with the frequency-dependent anomalous self-energy. Orange dashed stands for the conventional BdG assuming no frequency dependence of the order parameter. The inset shows the local density of states of the Green's function Eq. (1). The gap is chosen such that $\phi_0 = \omega_0/10$.

can be characterized by the probability for an electron to scatter into a hole-type excitation.

Within the BTK theory, the boundary condition (assumed to be at $z = 0$) is given by

$$\vec{\psi}_N(0) = \vec{\psi}_S(0), \tag{6}$$

$$\frac{\partial_z}{2m_N}\vec{\psi}_N(0) = \frac{\partial_z}{2m_S}\vec{\psi}_S(0) + H\vec{\psi}_S(0), \tag{7}$$

where m_S and m_N are the effective electron masses and H is the δ-barrier height. Performing the analytic continuation and replacing $i\epsilon_n \to \omega + i0^+$, the wave functions on superconducting side satisfy the equation $\hat{G}_{\mathbf{k}}^{-1}(\omega + i0^+)\vec{\psi}_S = 0$. On the normal side, the equation is the same with the substitution $\phi(\omega + i0^+) \to 0$ and $\mathcal{Z}(\omega + i0^+) \to 1$. In the following, we do not explicitly write 0^+ for shortness. The normal-state solution representing an incident electron and reflected electron and hole components is as follows:

$$\vec{\psi}_N = \begin{bmatrix}1\\0\end{bmatrix}e^{ik_e z} + \begin{bmatrix}r_N\\0\end{bmatrix}e^{-ik_e z} + \begin{bmatrix}0\\r_A\end{bmatrix}e^{ik_h z}, \tag{8}$$

where r_N and r_A denote the reflection amplitude in the electron and hole channels, respectively, and the electron/hole momenta are given by $k_{e/h} = \sqrt{2m(\mu \pm \omega)}$. Analogously, we find the solution for the quasielectrons and quasiholes propagating in the superconductor,

$$\vec{\psi}_S \approx C_{qe}\begin{bmatrix}1\\\eta_+\end{bmatrix}e^{ik_{qe}z} + C_{qh}\begin{bmatrix}1\\\eta_-\end{bmatrix}e^{-ik_{qh}z}, \tag{9}$$

where C_{qe} and C_{qh} are the corresponding amplitudes of the quasielectron and quasiholes and we denoted the corresponding coherence factors as $\eta_\pm = \phi(\omega)/[\mathcal{Z}(\omega)\omega \pm \sqrt{\mathcal{Z}^2(\omega)\omega^2 - \phi^2(\omega)}]$. In the quasiclassical limit, the quasielectron and quasihole momenta k_{qe}, k_{qh} can be taken to be equal to the corresponding Fermi momenta.

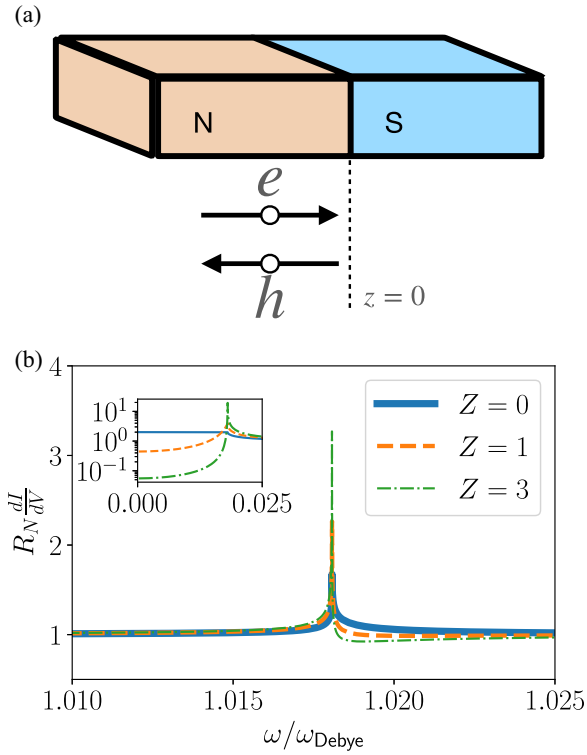

FIG. 3. (a) Schematic of the NS junction setup we consider in the BTK calculation. (b) Differential tunneling conductance as function of bias voltage (expressed in frequency units) for different values of the barrier height: $Z = 0$ solid blue, $Z = 1$ dashed orange, and $Z = 3$ dot-dashed green. The inset shows the same at low frequencies. The assumed electron-phonon coupling is $\lambda = 0.3$ (see the Supplemental Material [17]). The normal-state resistance is denoted as $R_N = (Z^2 + 1)/(2\nu_0 e^2 v_F \mathcal{A})$, where $\mathcal{A}$ is the contact surface area.

Upon solving the set of equations Eqs. (6)–(9) in the quasiclassical [20] limit and assuming $m_S = m_N$ we find the Andreev reflection coefficient to be as follows:

$$r_A = \frac{\eta_-\eta_+}{\eta_- + Z^2(\eta_- - \eta_+)}, \tag{10}$$

$$r_N = \frac{-Z(i+Z)}{\eta_- + Z^2(\eta_- - \eta_+)}(\eta_- - \eta_+), \tag{11}$$

where the normalized barrier height is defined as $Z \equiv mH/\sqrt{2m\mu}$. We note that the conventional Andreev reflection can be obtained from Eq. (10) by simply assuming frequency-independent $\mathcal{Z}$ and ϕ. In the limit of $\mathcal{Z} = 0$, the Andreev reflection coefficient is given by $r_A = \eta_+$. We, therefore, find that in order to have a strong Andreev reflection the condition $\phi \gg \mathcal{Z}\omega$ should be satisfied. The latter condition is always satisfied at very low frequencies leading to the conventional Andreev reflection [18] result $|r_A| \approx 1$. However, it can also be satisfied at large frequencies if the frequency-dependent order parameter $\Delta(\omega) \equiv \phi(\omega)/\mathcal{Z}(\omega)$ is larger than the frequency $\Delta(\omega) \gg \omega$. In this case, the reflection is up to a possible phase factor identical to the low-frequency case. As shown in Fig. 2, this scenario is realized for the Lorentz-like order parameter introduced above in the frequency range close to the resonance $\omega \sim \omega_0$.

II. FINITE-ENERGY BOUND STATES

We now consider the possibility of having the finite-energy Andreev bound states [18] in the junction consisting of two superconductors separated by a metallic region with the two boundaries located at $L/2$ and $-L/2$. We assume the phase difference between two superconductors to be γ. In order to find the bound states, we now follow the same procedure as for outlined above for the Andreev reflection but matching solutions at the two boundaries simultaneously. The general solution can be obtained analytically, but it is too cumbersome, and we, therefore, consider some simple limiting case. In particular, as we demonstrate in the Supplemental Material [17], in the limits $\phi_0 \ll \omega_0$ and $L \to 0$, there are two additional in-gap bound states $\omega \in [\omega_0, \omega_0 + \phi_0]$ with the frequencies ω_α (both positive and negative),

$$\omega_\alpha = \omega_0 + \frac{1}{2}\left\{1 + \alpha \cos\frac{\gamma}{2}\right\}, \tag{12}$$

with $\alpha = \pm$. We, thus, find the frequency of these bound states is of the order of the characteristic frequency of the order parameter frequency dependence. For both intrinsic and proximity superconductors, ω_0 can be expected to be on the order of several terahertz. This implies the existence of such bound states can potentially be probed by means of laser excitation. Their response is equivalent to a two-level system, thus, making them a good candidate for realization of solid state qubits.

III. INTERPRETATION AS DARK RESONANCE

We now discuss the interpretation of the additional Andreev reflection peak in terms of the so-called dark resonance. The concept of dark resonance is extensively studied within the field of quantum optics [12]. It is based on the existence of "slowly"-evolving superposition states in a quantum system, which are decoupled from the "fast," e.g., environment modes. For example, such optical phenomena as the electromagnetically induced transparency [11] are based on the existence of a dark resonance in a driven three-level system. The on-shell BdG Green's function Eq. (3), can be expressed as follows:

$$\hat{G}'^{-1}_{\mathbf{k}\to\mathbf{k}(\omega)}(\omega + i0^+) = \begin{pmatrix} \omega - \xi_\pm(\omega) & 0 & t & 0 \\ 0 & \omega + \xi_\pm(\omega) & 0 & -t \\ t & 0 & \omega & \omega_0 \\ 0 & -t & \omega_0 & \omega \end{pmatrix},$$

where $\xi_\pm(\omega) = \pm\sqrt{[(t^2-\omega^2)^2 - \omega^2\omega_0^2]/(\omega^2-\omega_0^2)}$ is the on-shell quasielectron and quasihole dispersions. By construction, the Green's function has the flat-band superconducting degree of freedom, which can be considered slow. By dark, we, thus, define states, which have projection onto the auxiliary degrees of freedom only. Let us now find the quasielectron and quasihole coherence vectors corresponding to the on-shell Green's function Eqs. (3) and (4). The latter is schematically shown in Fig. 1(c) in the limit of $t \to 0$. At frequencies $\omega \approx \omega_0$, one of the eigenstates of the auxiliary degrees of freedom crosses $\omega = 0$, therefore, being degenerate with the electron branch. The corresponding eigenvector is readily found to be given by $\approx [0, 0, 1, 1]^T/\sqrt{2}$. Thus, this vector only has slow nonpropagating (flat-band) components and are decoupled from the other degrees of freedom.

IV. EINSTEIN PHONON MODEL

Finally, we demonstrate that key results and conclusions of the toy model, involving the auxiliary superconductor, hold in the physical setup of interest where the pairing interaction is induced by the optical phonon mode. More specifically, we now consider the gap function induced by the interaction with the optical phonon mode with the propagator $\mathcal{D}_\mathbf{q}(i\nu_m) = -2\omega_0/(\omega_0^2 + \nu_m^2)$, where $\nu_m \equiv 2\pi m/\beta$, $m \in \mathbb{Z}$. As we demonstrate in the Supplemental Material [17], the matrix-valued self-energy $\hat{\Sigma}(i\epsilon_n)$ is found by solving the Dyson's equation. The latter reduces to two coupled equations for the inverse quasiparticle residue $\mathcal{Z}_n$, and the gap function ϕ_n in the case when the phonon propagator is momentum independent: $\hat{\Sigma}(i\epsilon_n) = (1-\mathcal{Z}_n)i\epsilon_n\hat{\tau}_0 + \phi_n\hat{\tau}_1$. The approximate analytical form of the phonon-induced self-energy can be obtained in the limit of weak electron-phonon coupling. As was shown in Refs. [6,7], the imaginary-axis dependence of the order parameter has the Lorentz form $\phi_n \propto \omega_0^2/(\omega_0^2 + \epsilon_n^2)$ and $\mathcal{Z}_n \approx 1$. This is, thus, in agreement with the assumed gap-frequency behavior in Eq. (1). At finite electron-phonon coupling strength, the gap frequency dependence deviates from the Lorentz form and additional resonances at frequencies $n\omega_0$ with $n = 1\text{–}3\cdots$ [7] emerge. However, the sharp features of the gap function, reminiscent to the pure Lorentz case, remain even at finite coupling strength [4,6,7]. We now study how these features affect the Andreev reflection from the NS boundary. More precisely, we consider the differential tunneling conductance, which expresses through the reflection coefficients Eqs. (10) and (11) as $dI/dV \propto 1 + |r_A|^2 - |r_N|^2$ [19]. Both reflection coefficients are found numerically by solving the complete set of Migdal-Eliashberg equations. The result of the numerical calculation is shown in Fig. 3 for different values of the barrier height Z. We find the prominent additional reflection peaks close to the Debye frequency, which correspond to the dark Andreev resonances. Note that the exact solution for the phonon case involves imaginary self-energy contributions, which give rise to a finite lifetime of the superconducting quasiparticles (absent in the toy model). However, these complications do not appear to affect the qualitative picture, and the signatures of the dark Andreev states are preserved.

V. CONCLUSIONS AND OUTLOOK

In this paper, we studied the quasiparticle properties of a superconductor with a frequency-dependent order parameter. When the latter has resonant features, we find an additional depletion of the high-energy density of states. We provide a physically equivalent two-band picture with an additional superconducting band gap emerging at high energies. For the NS junction, the band gap leads to additional Andreev reflection peaks at high energies. In the case of an *SNS* junction, we find Andreev bound states within the high-energy band gap. We provide an interpretation of these phenomena in terms of the dark resonance of the BdG Hamiltonian.We expect that the predicted phenomena should be accessible in experiments

with superconductors where the interaction is mediated by a well-localized bosonic, e.g., optical-phonon mode (for example, in MgB_2 [21], K_3C_{60} [22], etc.) and proximity systems involving flat-band and heavy-fermion materials [23]. We note that similar effects were observed in doped semiconductors, such as $SrTiO_3$ [24] where the interaction with phonons leads to the appearance of additional shadow/replica bands away from Fermi surface. The presence of these bands reveals itself in additional peaks in point-contact spectrum. This paper also suggests a number of follow-up ideas, at the intersection of superconductivity and quantum optics: e.g., the possibility of control of the dark Andreev states by external laser driving. Furthermore, it would be interesting to explore the role of frequency dependence of the order parameter on the quasiparticle spectrum in topological superconductors and whether dark Majorana-like states are possible.

ACKNOWLEDGEMENTS

This paper was supported by the National Science Foundation under Grant No. DMR-2037158, the US Army Research Office under Contract No. W911NF1310172, and the Simons Foundation. We are grateful to J. Sau for an illuminating discussion.

[1] J. Bardeen, L. N. Cooper, and J. R. Schrieffer, Phys. Rev. **108**, 1175 (1957).
[2] A. Altland and B. D. Simons, *Condensed Matter Field Theory* (Cambridge University Press, Cambridge, UK, 2010).
[3] G. Eliashberg, Sov. Phys. JETP **11**, 696 (1960).
[4] F. Marsiglio, Ann. Phys. (NY) **417**, 168102 (2020).
[5] F. Marsiglio, M. Schossmann, and J. P. Carbotte, Phys. Rev. B **37**, 4965 (1988).
[6] F. Marsiglio, Phys. Rev. B **98**, 024523 (2018).
[7] S. Mirabi, R. Boyack, and F. Marsiglio, Phys. Rev. B **101**, 064506 (2020).
[8] M. H. Christensen and A. V. Chubukov, Phys. Rev. B **104**, L140501 (2021).
[9] Y. G. Naidyuk and I. K. Yanson, *Point-Contact Spectroscopy*(Springer, Berlin, 2005), Vol. 145.
[10] W. L. McMillan and J. M. Rowell, Phys. Rev. Lett. **14**, 108 (1965).
[11] M. Fleischhauer and M. D. Lukin, Phys. Rev. Lett. **84**, 5094 (2000).
[12] M. D. Lukin, S. F. Yelin, M. Fleischhauer, and M. O. Scully, Phys. Rev. A **60**, 3225 (1999).
[13] M. Fleischhauer and M. D. Lukin, Phys. Rev. A **65**, 022314 (2002).
[14] J. R. Schrieffer, *Theory of Superconductivity* (CRC, Boca Raton, FL, 2018).
[15] A. V. Chubukov, A. Abanov, I. Esterlis, and S. A. Kivelson, Ann. Phys. (NY) **417**, 168190 (2020).
[16] C.-X. Liu, J. D. Sau, T. D. Stanescu, and S. Das Sarma, Phys. Rev. B **99**, 024510 (2019).
[17] See Supplemental Material at http://link.aps.org/supplemental/10.1103/PhysRevB.108.024501 or technical details such as the Green's function of the toy model, the gap function at weak coupling and the Andreev bound state energies.
[18] J. Sauls, Phil. Trans. A. Math. Phys. Eng. Sci. **376** (2018).
[19] G. E. Blonder, M. Tinkham, and T. M. Klapwijk, Phys. Rev. B **25**, 4515 (1982).
[20] W. Belzig, F. K. Wilhelm, C. Bruder, G. Schön, and A. D. Zaikin, Superlattices Microstruct. **25**, 1251 (1999).
[21] I. I. Mazin, O. K. Andersen, O. Jepsen, O. V. Dolgov, J. Kortus, A. A. Golubov, A. B. Kuz'menko, and D. van der Marel, Phys. Rev. Lett. **89**, 107002 (2002).
[22] F. C. Zhang, M. Ogata, and T. M. Rice, Phys. Rev. Lett. **67**, 3452 (1991).
[23] L. Balents, C. R. Dean, D. K. Efetov, and A. F. Young, Nat. Phys. **16**, 725 (2020).
[24] J. J. Lee, F. T. Schmitt, R. G. Moore, S. Johnston, Y. T. Cui, W. Li, M. Yi, Z. K. Liu, M. Hashimoto, Y. Zhang, D. H. Lu, T. P. Devereaux, D. H. Lee, and Z. X. Shen, Nature (London) **515**, 245 (2014).